

LIRONG YANG<sup>1</sup>, HUI YANG<sup>2</sup>

## Load identification method of ball mill based on the CEEMDAN-wavelet threshold-PMMFE

### Introduction

Ball mill plays a vital role in the grinding operation and the mill will inevitably bear the workload during operation. The mill load can thus be considered to be an important parameter that directly affects the grinding effect and grinding efficiency (Tang et al. 2013). Due to the complex and changeable working environment inside the cylinder during the grinding process, the problem of difficult load identification of ball mills is common in current grinding operations (Tang et al. 2011; Zhao et al. 2017). The commonly used method is to take the vibration signal of the mill bearing, cylinder, base and other parts as the research object (Tang et al. 2012), and realize the load state identification of the ball mill by analyzing the relationship between the vibration signal characteristics and the load of the ball mill.

✉ Corresponding Author: Lirong Yang; e-mail: 18978844@qq.com

<sup>1</sup> Jiangxi Mining and Metallurgical Engineering Research Center, China; School of Mechanical and Electrical Engineering, Jiangxi University of Science and Technology, Ganzhou, Jiangxi Province, China; e-mail: 18978844@qq.com

<sup>2</sup> School of Mechanical and Electrical Engineering, Jiangxi University of Science and Technology, Ganzhou, Jiangxi Province, China; ORCID iD: 0009-0001-6736-7638; e-mail: 1850881582@qq.com



At the same time, in view of the characteristics of vibration signals of ball mills and the limitations of current commonly used signal processing methods, Luo Xiaoyan et al. (2016) proposes a new idea of wavelet analysis applied to the extraction of vibration signal characteristics of mill bearings. Tang Jian et al. (2014) introduces the EMD algorithm to analyze the vibration signal of mill, and combines multi-scale spectrum and partial least squares algorithm to establish a soft measurement model to successfully identify the grinding load. Zhao Lijie (2014) introduces the EEMD algorithm into the vibration signal processing procedure of the ball mill; The above method has certain effects in feature extraction and load identification, but the high-dimensional spectral features make the establishment of a load-identification model difficult. The determination of the optimal parameters of wavelet analysis will affect the accuracy of the identification of the load state of the ball mill. Both the EMD algorithm and the EEMD algorithm have modal aliasing in the process of signal decomposition, resulting in unsatisfactory modeling accuracy.

Complete ensemble empirical mode decomposition with adaptive noise (CEEMDAN) can obtain the IMF component by EMD decomposition of the added Gaussian white noise during the decomposition process (Torres et al. 2011), replacing the Gaussian white noise added each time during the EEMD decomposition process to achieve adaptive addition noise. This method not only makes up for the shortcomings of the modal aliasing of EMD algorithm and the EEMD algorithm but also improves the completeness of decomposition; however, there is a defect of discarding components in the process of CEEMDAN denoising. Cai Gaipin et al. (2019) for the ball mill cylinder vibration signal nonlinearity, non-smoothness characteristics, as well as the shortcomings of CEEMDAN denoising, proposed a CEEMDAN-wavelet threshold joint denoising method, and through the measured signals to verify the effectiveness of the method.

Fuzzy entropy (FE) is a measure of discrete time series complexity and has been widely used in the fault diagnosis of rotating machinery equipment (Chen Weiting et al. 2009; Zheng Jinde et al. 2016). Multi-scale fuzzy entropy (MFE) is a calculation of fuzzy entropy values for discrete time series at multiple scales (Wang Hongjun et al. 2019), which has better anti-interference ability and adaptability than fuzzy entropy. Yang Wangcan et al. proposed a fault diagnosis method based on EEMD multi-scale fuzzy entropy (Yang Wangcan et al. 2015) and proved that the method can effectively improve the fault diagnosis accuracy by analyzing the fault results. Li Baoqing et al. combined the adaptive sparsest time-frequency analysis method with multi-scale fuzzy mean entropy (PMMFE) to analyze gear faults to realize the identification of gear faults (Li Baoqing et al. 2016). Although some scholars in China have achieved good results in applying multi-scale fuzzy entropy partial mean to the fault diagnosis of rotating machinery, there are few studies on its application with regard to mill load identification.

Combined with the superiority of the CEEMDAN-wavelet threshold combined denoising method and the strong anti-interference ability of PMMFE, a load identification method for ball mill based on CEEMDAN-wavelet threshold-PMMFE is proposed. At the same time, the least squares support vector machine (LSSVM) algorithm is introduced to identify the load of the feature vector composed of entropy features (Chang Yufang et al. 2013; Wang

et al. 2023) and the recognition accuracy of the method is observed. Through the vibration signal analysis of the measured mill, the proposed method is compared with the single fuzzy entropy feature, multi-scale fuzzy entropy feature and multi-scale fuzzy entropy partial mean feature by LSSVM algorithm for load identification, and the results show that the proposed method has the highest load recognition accuracy.

## 1. Basic principle

### 1.1. CEEMDAN-wavelet threshold combined denoising method

In the process of denoising, the CEEMDAN-wavelet threshold combined denoising method only denoises the high-frequency IMF components with more noise instead of the entire signal (Donoho et al. 1994; Zheng Jinde 2014). Therefore, while achieving the purpose of eliminating noise, the useful features in the signal are well retained. Its main steps are as follows.

1.  $I$ -th experiments were performed on the noisy signal  $x(t) + \varepsilon^0 v^j(t)$ , and  $\widehat{IMF}_1(t)$  was obtained by EMD.

$$\widehat{IMF}_1(t) = \frac{1}{I} \sum_{i=1}^I IMF_1^i(t) \quad (1)$$

2. The only margin signal when  $k = 1$  is calculated.

$$r_1(t) = x(t) - \widehat{IMF}_1(t) \dots \quad (2)$$

3. Then perform the  $i$ -th experiment ( $i = 1, \dots, I$ ), in each experiment, the signal  $r_i(t) = \varepsilon_1 E_1(v^j(t))$  is decomposed until the first modal component is obtained, and the calculation of the second modal component begins.

$$\widehat{IMF}_2(t) = \frac{1}{I} \sum_{i=1}^I E_1(r_1(t)) + \varepsilon_1 E_1(v^j(t)) \quad (3)$$

4. For the remaining stages, i.e.  $k = 2, \dots, K$ , in line with the calculation process in Step 3, the  $k$ th residual signal is calculated first, and then the  $k + 1$  st modal component is calculated.

$$r_k(t) = r_{k-1}(t) - \widehat{IMF}_k(t) \quad (4)$$

$$\widehat{IMF}_{k+1}(t) = \frac{1}{I} \sum_{i=1}^I E_1(r_k(t)) + \varepsilon_k E_k(v^j(t)) \quad (5)$$

- Repeat Step 4 until the number of poles of the obtained margin signal is less than two, and the algorithm ends. At this point, the number of all modal functions is  $k$ , and the original signal sequence  $x(t)$  is decomposed into the following:

$$x(t) = \sum_{k=1}^K \widehat{IMF}_k + R(t) \quad (6)$$

- The continuous mean squared error criterion is used to determine the high-frequency IMF component with more noise in the decomposed IMF component and select the parameters of the appropriate wavelet to denoise the high-frequency IMF component with more noise.
- The denoising IMF component and the undenoising IMF component were reconstructed to obtain the signal  $x'(t)$  after denoising by the joint denoising method.

In the above equations:  $EK(\cdot)$ : the  $k$ -th modal component obtained by EMD decomposition;  $\widehat{c}_k(t)$ : the  $k$ -th modal component produced by CEEMDAN;  $v^i$ : Gaussian white noise obeying  $n$ ;  $\varepsilon$ : The standard deviation of white Gaussian noise.

## 1.2. PMMFE algorithm

Multi-scale fuzzy entropy is developed based on multi-scale entropy on the basis of fuzzy entropy and the process is to coarse-grain the original time series, construct a multi-scale time series, and then calculate the fuzzy values at each scale. For a time series  $X = \{x(i), i = 1, 2, \dots, N\}$  the specific steps are as follows:

- Given the embedding dimension  $m$  and similar volume  $r$  in advance, the time series  $X = \{x(i), i = 1, 2, \dots, N\}$  is coarse-grained to obtain the processed coarse-grained sequence:

$$y^s(j) = \frac{1}{s} \sum_{i=(j-1)s+1}^{js} x(i) \quad 1 \leq j \leq \frac{N}{s} \quad (7)$$

↳  $s$  – scale factor;

$y_s(j)$  – time series under different scale factors.

- Calculate the fuzzy entropy of each coarse-grained sequence and reduce it as a function of the scale factor  $s$ . When calculating the fuzzy entropy for each coarse-grained sequence, the similar volume  $r$  is unchanged, usually  $r$  takes  $0.1 \sim 0.25SD$  ( $SD$  is the standard deviation of the original signal).

Multi-scale fuzzy entropy partial mean is a kind of characteristic value based on multi-scale fuzzy entropy that reflects the trend of signal fuzzy entropy with scale change and the nonlinear information of time series at multiple scales; its calculation formula is as follows:

$$PMMFE = (1 + |ske(MFE)/3|) \cdot mean(MFE) \quad (8)$$

- ↪  $MFE$  – multi-scale fuzzy entropy of the signal under a certain time-scale factor  $s$ .  
 $ske(MFE)$  – skewness of the multiscale fuzzy entropy value.

### 1.3. LSSVM algorithm

The least squares support vector machine (LSSVM) is an improved algorithm of a support vector machine (SVM) based on statistical theory, which uses the least squares method to solve the model parameters, which effectively improves the computational efficiency; its main steps are as follows:

1. Processed for a given set of training samples  $S = \{(x_1, y_1), (x_2, y_2), \dots, (x_n, y_n)\}$  and assuming a model.

$$f(x) = w^T \cdot \mathcal{O}(x) + b \quad (9)$$

- ↪  $x$  – input feature vector;  
 $\mathcal{O}x$  – mapping function that maps the input samples to the high-dimensional feature space;  
 $w$  – weight vector corresponding to the feature vector, and  $b$  is the bias term.
2. Find a hyperplane such that all sample points are as close as possible to this hyperplane, and then solve for the hyperplane parameters by minimizing the following optimization problem.

$$\begin{cases} \min \left[ \frac{1}{2} w^T w + \frac{1}{2} C \sum_{i=1}^n e_i^2 \right] \\ \text{s.t. } y_i = w \cdot \mathcal{O}(x) + b + e_i \end{cases} \quad (10)$$

- ↪  $e_i$  – relaxation variable;  
 $C$  – regularization parameter.
3. Introduce the Lagrange multiplier and derive it so that its derivative is zero.
  4. Eventually, the LSSVM regression function can be built.

$$f(x) = \sum_{i=1}^n \alpha_i k(x_i, x) + b \quad (11)$$

- ↪  $\alpha_i$  – Lagrange multiplier;  
 $k(x_i, x)$  – kernel function.

### 1.4. ReliefF algorithm

The ReliefF weighted feature selection algorithm is an improved method of feature selection that can deal with multiclassification problems in view of the limitation that the Relief algorithm can only be applied to the selection of features for two types of data, and was proposed by Kononeill in 1994 (Kononerko 1994). It calculates the weights of the feature parameters and judges the correlation between the feature parameters and the categories according to the size of the weights. Its specific implementation steps are as follows:

Input: training sample set  $D$ , number of iterations  $m$ , number of nearest neighbour samples  $k$ ;

Output: vector of weights  $w$  for each feature parameter.

1. Initialisation:  $w = 0$ ;
2. Arbitrarily select a sample  $R$  among the feature matrix samples and find the  $k$  nearest-neighbour samples  $H_i$  of the same class as it and the  $K$  nearest-neighbour samples  $M_i$  ( $i = 1, 2, 3, \dots, k$ ) of a different class, respectively;
3. For all feature samples  $F_j$  ( $j = 1, 2, 3, \dots, J$ ) of sample  $R$  in turn, update the weights of each feature parameter;

$$W(F_j) = W(F_j) - \sum_{i=1}^k \text{diff}(F_j, R, H_i) / k + \sum_{i=1}^k \text{diff}(F_j, R, M_i) / k \quad (12)$$

$$\text{diff}(F_j, R, H_i) = \left| \text{Value}(F_j, R) - \text{Value}(F_j, H_i) \right| / \left( \max(F_j) - \min(F_j) \right) \quad (13)$$

$$\text{diff}(F_j, R, M_i) = \left| \text{Value}(F_j, R) - \text{Value}(F_j, M_i) \right| / \left( \max(F_j) - \min(F_j) \right) \quad (14)$$

↳  $\text{Value}(M_i, A)$  – value of the  $j$ -th feature of sample  $A$ ;

$A$  – can be taken as  $R, H_i$  or  $M_i$ ;

$\text{diff}$  – Euclidean distance between two samples.

4. Cycle Steps (1) to (3)  $m$  times, i.e., randomly select  $m$  samples for the computation of weight vectors, so as to obtain the weight vectors  $w$  of each feature parameter.

## 2. Experimental analysis of mill load characteristic extraction

### 2.1. Ball mill bearing vibration signal collection

In this experiment, the Bond index ball mill with a model of  $\Phi 305 \times 305$  mm was used as the object to simulate the grinding operation, and the vibration signal acquisition system

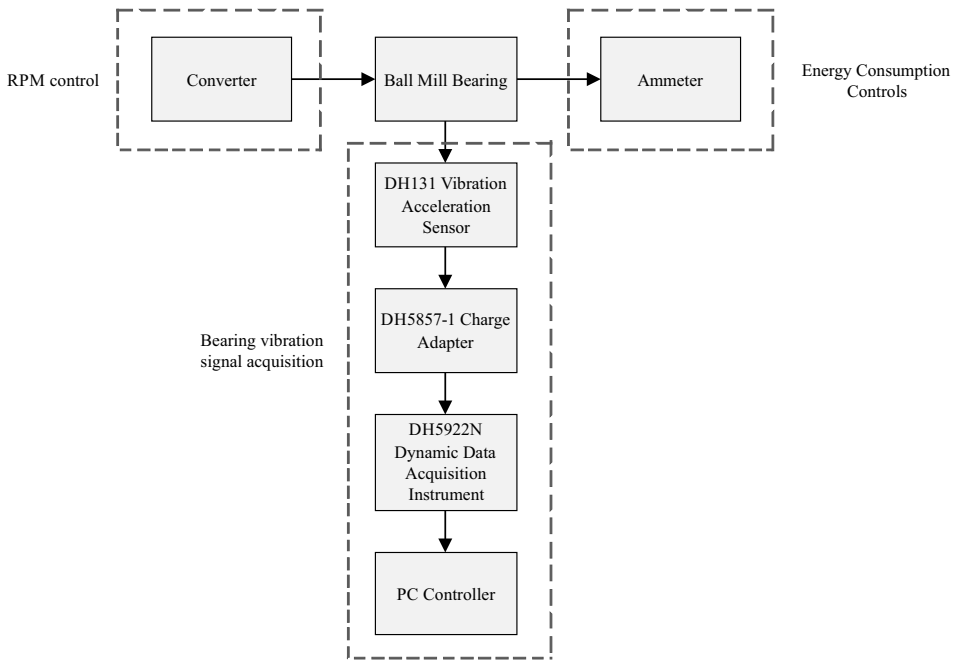


Fig. 1. Bearing vibration signal acquisition system block diagram

Rys. 1. Schemat blokowy systemu akwizycji sygnału drgań łożyska

was built according to the existing conditions of the laboratory. Among them, the bearing vibration signal acquisition system is mainly composed of a DH5922N dynamic data collector, a DH131 vibration acceleration sensor, a DH5857-1 charge adapter, a frequency converter, an energy meter and a PC, and the structural block diagram of the vibration signal acquisition system is shown in Figure 1.

Ten sets of vibration signals of bearings under three conditions of underload, normal load and overload of ball mill were collected, and the sampling frequency during the acquisition process was 20kHz, and the acquisition time was set to 10 min as well as the grinding time. The intervals of the three load divisions are: underload ( $\emptyset \leq 0.2$ ;  $\emptyset = 0.3$ ,  $\Psi < 0.6$ ), normal load ( $\emptyset = 0.3$ ,  $0.6 \leq \Psi \leq 1.2$ ;  $\emptyset = 0.4$ ,  $0.5 \leq \Psi \leq 0.9$ ), overload ( $\emptyset = 0.4$ ,  $0.9 < \Psi$ ;  $0.5 \leq \emptyset$ ), where  $\emptyset$  represents the filling rate and  $\Psi$  represents the ratio of the material to the ball.

In the grinding experiment, the speed of the ball mill is set to 48 r/min, and it is known that the time required for the cylinder to rotate for one week is about 1.25 s. In the process of signal processing analysis, in order to ensure that the signal characteristic parameters can fully reflect the load of the ball mill, the length of the signal processing analysis selects the sampling signal of the ball mill running for about eight cycles, and the bearing vibration signal with a duration of about 10s to ensure the reliability of the characteristic parameters obtained during the signal analysis process. The waveform diagram of the vibration signal of the ball mill bearing under three different load parameters is as shown in Figure 2.

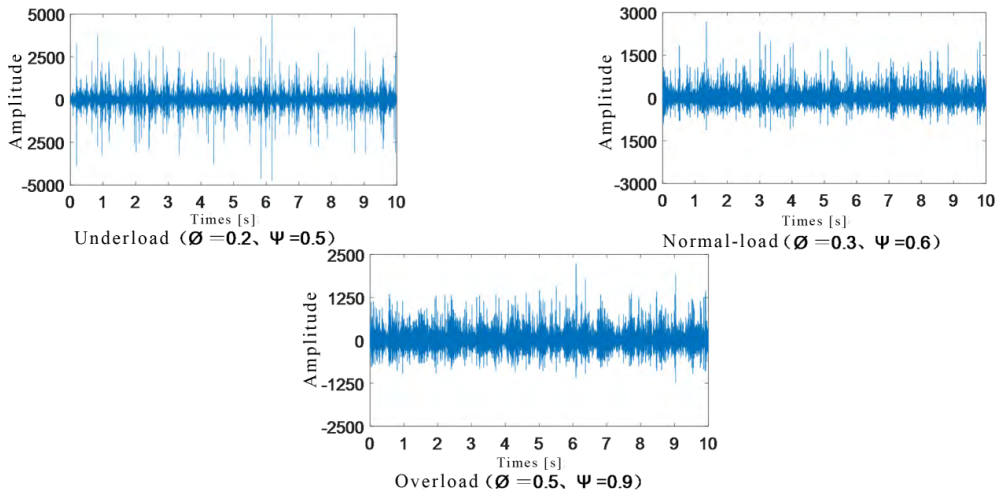


Fig. 2. The raw signals under the three load conditions

Rys. 2. Surowe sygnały w trzech warunkach obciążenia

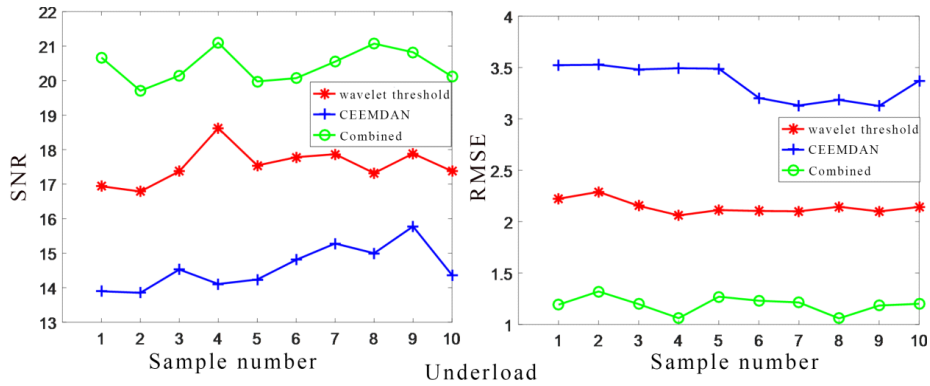
From the vibration signal waveform in Figure 2, it can be seen that it is difficult to accurately distinguish the load state of the ball mill only by relying on the difference in amplitude in the waveform diagram. Therefore, it is very important to denoise the vibration signal of the ball mill bearing and identify the load state of the ball mill according to the difference in the characteristic signal extracted after denoising.

## 2.2. Joint denoising method and effect analysis

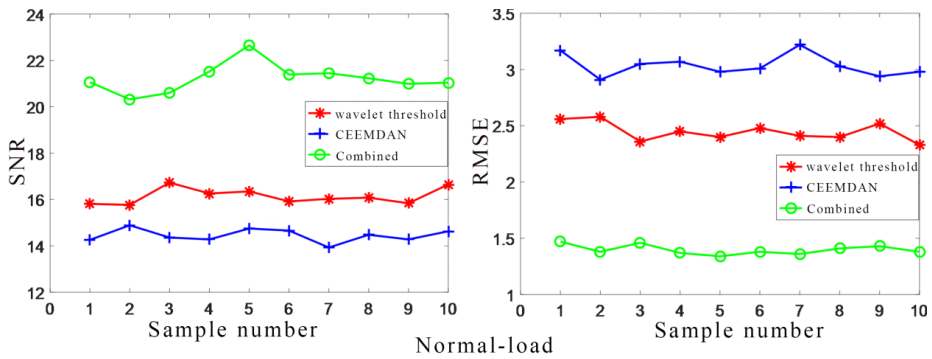
Due to the wide frequency range of vibration signals generated during the grinding process, and because the vibration signal of the pure ball mill barrel is unknown, the signal-to-noise ratio and rms error are used as the indicators to judge the denoising effect and the denoising effects of different denoising methods are compared. The wavelet parameters in the denoising process are set as follows: the wavelet basis function is db8, the number of decomposition layers is 5, the heursure criterion is adopted, and the hard threshold is used. The signal-to-noise ratio and root mean square error of the bearing vibration signal after denoising the bearing vibration signal by CEEMDAN denoising, wavelet threshold denoising and CEEMDAN-wavelet threshold combined denoising are shown in Figure 3.

It can be seen from the denoising results in Figure 3 that when the denoising method is the same, the evaluation index change of noise effect under the same load state is small and the evaluation index change of noise effect under adifferent load states is quite different.

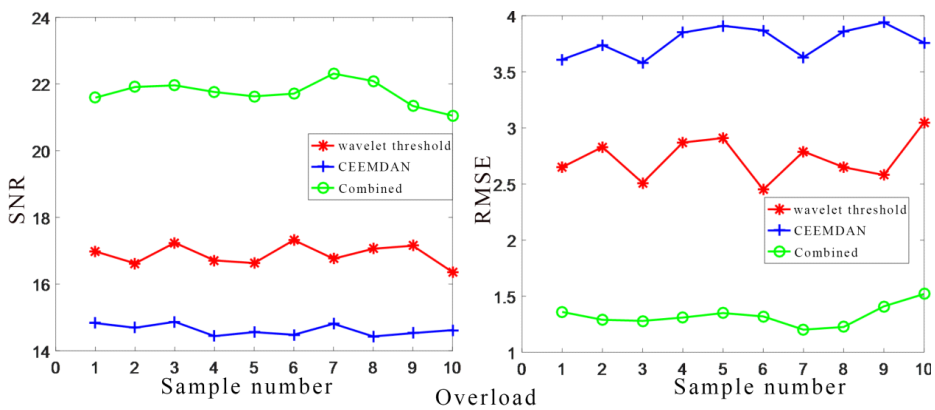




(a) underload status



(b) normal load status



(c) overload status

Fig. 3. The results of three different denoising methods

Rys. 3. Wyniki trzech różnych metod odszumiania

When the load state is the same, the denoising effect of different denoising methods is different, and the signal after CEEMDAN-wavelet threshold combined with denoising has the largest signal-to-noise ratio and the smallest rms error value.

According to the criteria of the signal-to-noise ratio and rms error to evaluate the denoising effect, it can be seen that the CEEMDAN-wavelet threshold combined with denoising has the best effect, and the CEEMDAN alone has the worst denoising effect. It shows that the wavelet threshold denoising method and CEEMDAN denoising method alone lose some effective information in the process of noise reduction, while the combined denoising method retains the effective information in the signal to the greatest extent while reducing noise.

### 2.3. Feature extraction and analysis of entropy

Firstly, the ability to distinguish different load states of the mill with fuzzy entropy as a characteristic index is analyzed. Thirty sets of experimental data are denoised; Then, in accordance with the fuzzy entropy calculation step, the fuzzy entropy of each group of samples under the load state of three different mills is obtained. In the process of calculating fuzzy entropy, the embedding dimension  $m$  and the similar tolerance  $r$  are important factors affecting the entropy value.

The value of the embedding dimension  $m$  is too small, there are fewer features in the reconstructed signal contained in the signal and the algorithm fails. The value of the embedding dimension  $m$  is too large, the data length required for calculation is longer, and the features contained in the reconstruction signal are too redundant, which is not easy to distinguish the change of the signal, and also increases the amount of calculation. Usually, the relationship between data length  $N$  and embedding dimension  $m$  is  $N = 10^m \sim 30^m$ , but in this paper, the data length is selected as 200,000 in the analysis process, so  $m = 6$  is considered comprehensively.

The similarity tolerance  $r$  indicates the width of the fuzzy function boundary. If  $r$  is too big, a lot of statistical information will be lost; if  $r$  is too small, the estimated statistical characteristics are not ideal and there is an increase in sensitivity to the resulting noise. Therefore,  $r$  generally takes  $0.1 \sim 0.25$  SD (SD is the standard deviation of the original data), and in this paper, we take  $r = 0.15$  SD.

The distribution of fuzzy entropy values under different load conditions is shown in Figure 4.

From Figure 4, the fuzzy entropy values of ball mill vibration signals under different load states have different fluctuation intervals and fluctuation amplitudes. The fuzzy entropy value as a feature can distinguish the normal load and abnormal load state, but the ball mill grinding is a continuous process, and the underload and overload state under abnormal load have different load parameters to be adjusted, and improper operation will not only reduce the efficiency of grinding but will also cause production accidents in serious cases.

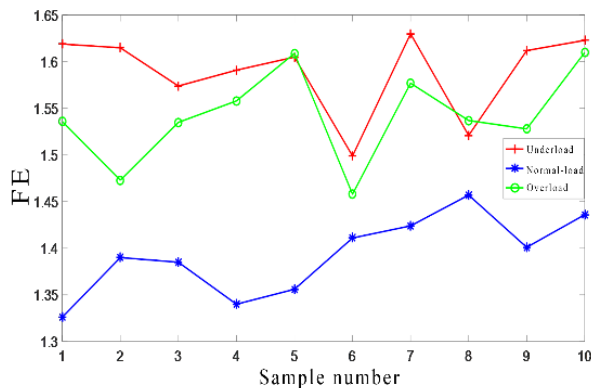


Fig. 4. The fuzzy entropy value of experimental data in different load conditions

Rys. 4. Wartość entropii rozmytej danych eksperymentalnych w różnych warunkach obciążenia

Therefore, the direct use of fuzzy entropy as the eigenvalue of ball mill load state identification may be a cause of misjudgment.

In view of the fact that it may be difficult to accurately judge the load state of the ball mill by using a single fuzzy entropy value as the eigenvalue of the bearing vibration signals, multiscale fuzzy entropy is used as the eigenvalue to analyze the load of the mill. The embedding dimension  $m = 6$ , the similarity tolerance  $r = 0.15$  SD, and the maximum scale factor  $s = 15$  are adopted in the calculation process. Limited to space, the multiscale fuzzy entropy values of three groups of signals are selected for each load state and the results are shown in Figure 5.

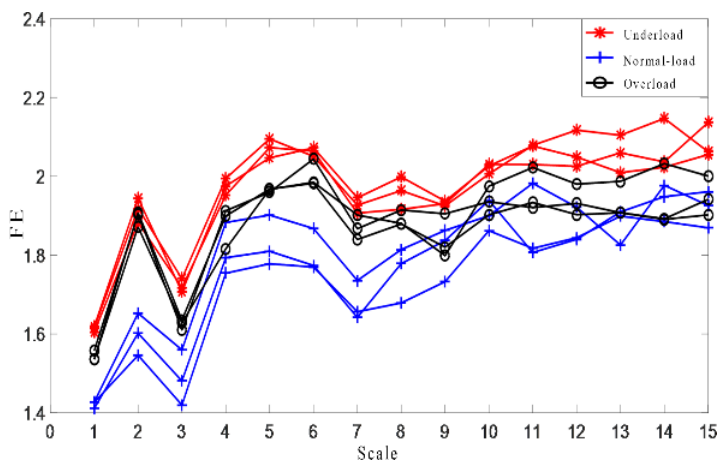


Fig. 5. The MFE of vibration signal under different load conditions

Rys. 5. MFE sygnału drgań w różnych warunkach obciążenia

As can be seen from the change curves in Figure 5, although the overall trend of the fuzzy entropy value of the vibration signals with the scale factor under different load states is consistent overall, the change intervals of the entropy value are different. Furthermore, the fluctuation zone of the multi-scale fuzzy entropy value under the overload state has no obvious boundaries compared with the fluctuation zones under the other two load states, and there is some overlap and crossover. Therefore the direct adoption of multi-scale fuzzy entropy as the eigenvalue of ball mill load state identification may be a source of misjudgment.

In order to comprehensively analyze the complexity and randomness of mill vibration signals on different scales, the multiscale fuzzy entropy partial mean values of vibration signals under different load states are calculated respectively, in which twenty groups of signals are selected for analysis under each load state and the results are shown in Figure 6.

As can be seen from Figure 6, there are some differences in the distribution of multi-scale fuzzy entropy of ball mill vibration signals in different loading states. The multi-scale fuzzy entropy of ball mill bearing vibration signals in the under-loaded state is the largest, the multi-scale fuzzy entropy of bearing vibration signals in the over-loaded state is the smallest, and the multi-scale fuzzy entropy of normal loading state ball mill bearing vibration signals is relatively moderate. Moreover, the difference of the partial mean value under similar load condition is small, and the difference of the partial mean value under different load conditions is large. Comparing Figure 5 and 6, it can be observed that the fluctuation amplitude of multi-scale fuzzy entropy partial mean values under different load states is smaller compared with that of multi-scale fuzzy entropy values and the boundaries of fluctuation intervals are more obvious.

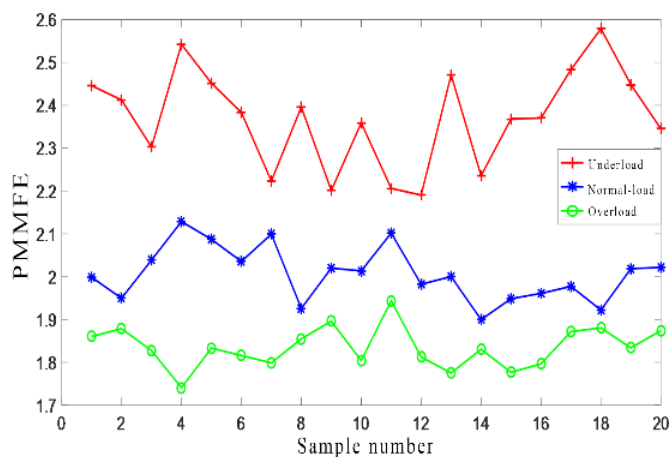


Fig. 6. The PMMFE of experimental data under different load conditions

Rys. 6. PMMFE danych eksperymentalnych w różnych warunkach obciążenia

### 3. Construction of feature vectors and the identification of mill load states

#### 3.1. Construction of eigenvector

Grinding is a nonlinear, strongly coupled and complex process, and there may be some option to identify the mill load state by using the multiscale fuzzy entropy skewed mean value as the mill load eigenvalue alone (Ren Weihe et al. 2023; Zhu Jin et al. 2023). Therefore, in order to accurately identify the ball mill load state, the ReliefF weighted feature selection algorithm is used to select two fuzzy entropy values with higher sensitivity to the mill load from the multiscale fuzzy entropy values, and combined with the multiscale fuzzy entropy skewed mean value, a three-dimensional mill load eigenvector is jointly constructed.

The sample set consists of fifteen entropy value feature parameters of the vibration signals of mill bearings under three different types of load (underload, normal load, overload) states together, twenty groups of samples for each load state, and the feature data is fifteen dimensions, which constitutes a  $60 \times 15$  dimensional feature set inputted into ReliefF weighted feature selection algorithm. The weighting values between the fuzzy entropy and the load categories under each scale factor in the multi-scale fuzzy entropy value were obtained and the results are shown in Figure 7.

As can be seen from Figure 7, the weight value of the fuzzy entropy value in the multi-scale fuzzy entropy value when the scale factor is 3 and 5 is larger, which is 0.4207 and 0.4342, respectively, indicating that the fuzzy entropy value of the multi-scale fuzzy entropy value under the scale factor of 3 and 5 has a higher sensitivity to the change of the state

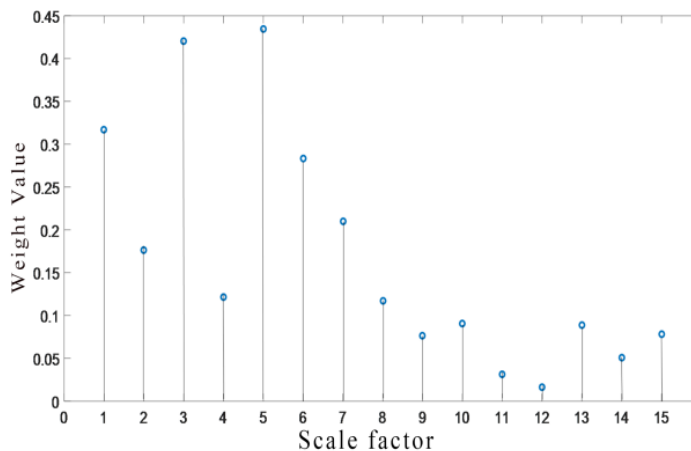


Fig. 7. ReliefF algorithm calculates the weights of the fuzzy entropy under the scale factors of vibration signals

Rys. 7. Algorytm ReliefF oblicza wagi entropii rozmytej w ramach współczynników skali sygnałów drganiowych

of the mill load. In order to reduce the amount of computation in the process of load identification, the fuzzy entropy value and the multiscale fuzzy entropy bias mean value of the multiscale fuzzy entropy value at scale factor 3 and 5 are selected as the eigenvalues of the mill load to construct the eigenvectors for the mill load identification, and the obtained eigenvectors are as follows: Multi-scale fuzzy entropy value with scale factor 3, Multi-scale fuzzy entropy value with scale factor 5, Multi-scale fuzzy entropy skewed mean value.

### 3.2. Mill load state identification

In order to verify the feasibility of the constructed feature vectors, the mill load feature vectors are used as the input of the LSSVM algorithm, and the mill load state is used as the output to establish the mill load recognition model.

In the process of load recognition, thirty groups of vibration signals are selected for each mill load state for mill load feature vector extraction, and a  $90 \times 3$  dimensional feature vector matrix is constructed in which fifteen groups are selected for each load state as test samples and the remaining samples are recognized as test samples. In order to verify the effect of the denoising effect and the influence of feature parameters on the accuracy of load recognition, the feature vectors obtained by different denoising methods are recognized using the LSSVM algorithm, and the load recognition results of different methods are obtained as shown in Table 1.

As can be seen from Table 1, comparing the load recognition results of serial numbers 1, 2, 3 and 4, the accuracy of direct recognition of the original vibration signal features is the lowest. The accuracy of mill load recognition is the highest after using the joint CEEMDAN-wavelet thresholding method of denoising the vibration signals, and the accuracy of the recognition is increased by 22.2%, 17.7% compared to that of the denoising

Table 1. The recognition results of eigenvectors obtained by different methods

Tabela 1. Wyniki rozpoznawania wektorów własnych uzyskane różnymi metodami

Number	Denoising methods	Parameterization	Load identification methods	Load identification accuracy
1	Original signal	eigenvectors (scale because of fuzzy entropy values of 3, 5 and PMMFE)	LSSVM	62.2%
2	CEEMDAN			66.7%
3	Wavelet threshold			71.1%
4	CEEMDAN-wavelet threshold			84.4%
5	CEEMDAN-wavelet threshold	FE		46.7%
6	CEEMDAN-wavelet threshold	MFE		57.8%

methods used in serial numbers 1, 2 and 3, respectively, 13.3%; and with the improvement of the denoising effect, the accuracy of mill load recognition also increases.

Comparing the load recognition results of serial numbers 4, 5 and 6, it can be seen that when the denoising methods are the same, the load recognition accuracy of the feature vector constructed in this paper is the highest, the accuracy of which reaches 84.4%. The load recognition accuracy of the fuzzy entropy value as the feature parameter is the lowest, which indicates that the selection of feature parameters is a key factor affecting the accuracy of the mill load recognition.

Comprehensive comparison of the above analysis results shows that the accuracy of the ball mill load identification method based on CEEMDAN-wavelet threshold and multi-scale fuzzy entropy proposed in this paper is the highest, which indicates that the feature vectors constructed in this paper can effectively characterize the load characteristics of the mill, and also verifies the effectiveness of the method used in this paper.

## Conclusions

1. Aiming at the situation that there is a large amount of noise in the original signal, CEEMDAN, wavelet threshold denoising and CEEMDAN-wavelet threshold joint denoising methods are used to denoise and analyze the vibration signals under different loading conditions.
2. The PMMFE algorithm is proposed for feature extraction after signal preprocessing. The relationship between the fuzzy entropy, MFE and PMMFE of vibration signals and mill load is analyzed, and the results show that PMMFE can distinguish the three load states more accurately compared with fuzzy entropy and MFE.
3. For the CEEMDAN-wavelet threshold joint denoising method proposed in this paper and the CEEMDAN denoising and wavelet threshold denoising methods commonly used in mills, the LSSVM algorithm is introduced to compare the difference in the accuracy rate of mill load recognition caused by different methods. The results show that the recognition accuracy of the proposed CEEMDAN-wavelet thresholding joint denoising method is 84.4%, which improves the recognition accuracy by 17.7% and 13.3% over the CEEMDAN and wavelet thresholding methods, respectively.
4. Comparison of the recognition accuracy of mill loads by different feature parameter methods through the LSSVM algorithm shows that the result of feature vector recognition strongly depends on the method of feature parameter selection. In the same case of CEEMDAN-wavelet threshold joint denoising, the recognition accuracy with PMMFE as the feature parameter is 84.4%, which is 37.7% and 26.6% higher than that with fuzzy FE or MFE as the feature parameter, respectively.

*This work was supported by the General Project of Ganzhou Key R&D Programme (grant number 20210112411).*

## REFERENCES

- Cai et al. 2017 – Cai, G., Zhao, X., Hu, X., Huang, X. and Chen, H. 2020. Denoising Method of Vibration Signal of Ball Mill based on CEEMDAN-wavelet Threshold Combination. *Mechanical Science and Technology for Aerospace Engineering* 39(7), pp. 1077–1085, DOI: 10.13433/j.cnki.1003-8728.20190241.
- Chang et al. 2023 – Chang, Y., Zhu, Z., Tang, Y., et al. 2023. Wind power prediction model based on CEEMD and improved SSA-LSSVM. *Sensors and Microsystems* 42(10), pp. 130–134.
- Chen et al. 2009 – Chen W., Jun, Z., Yu, W. and Wang, Z. 2009. Measuring complexity using FuzzyEn, ApEn, and SampEn. *Medical Engineering and Physics* 31(1), pp. 61–68, DOI: 10.1016/j.medengphy.2008.04.005.
- Donoho, D.L. and Johnstone, I.M. 1994. Ideal Spatial Adaptation by Wavelet Shrinkage. *Biometrika* 81(3), pp. 425–455, DOI: 10.1093/biomet/81.3.425.
- Kononerko, I. 1994. *Estimating attributes: analysis and extension of Relief*. [In:] *Proceedings of European conference on machine learning*, Springer-Verlag New York, pp. 171–182.
- Li et al. 2016 – Li, B., Cheng, J., Wu, Z., et al. 2016. Gear fault diagnosis method based on the adaptive and sparsest time-frequency analysis method and partial mean multi-scale fuzzy entropy. *Journal of Vibration Engineering* 29(5), pp. 928–935.
- Luo et al 2016 – Luo, X., Lu, X., Yang, X., et al. 2016. Feature Extraction Method for Ball-mill Bearing's Vibration Signals Using Wavelet Analysis. *Noise and Vibration Control* 36(1), pp. 148–152.
- Ren et al 2023 – Ren, W., Zan, L. and Li, X. 2023. Coherent orthogonal frequency division multiplexing passive optical network system based on eigenvector construction. *Laser Journal* 44(3), pp. 195–199.
- Tang et al. 2011 – Tang, J., Zhao, L.J., Yue, H., Yu, W. and Chai, T. 2011. Vibration analysis based on empirical mode decomposition and partial least squares. *Procedia Engineering* 16(1), pp. 646–652, DOI: 10.1016/j.proeng.2011.08.1136.
- Tang et al. 2012 – Tang, J., Chai, T., Zhao L.J., Yue, H. and Zheng, X.P. 2012. Ensemble modeling for parameters of ball-mill load in grinding process based on frequency spectrum of shell vibration. *Control Theory and Application* 29(2), pp. 183–191.
- Tang et al. 2013 – Tang, J., Chai, T., Yu, W. and Zhao, L.J. 2013. Modeling load parameters of ball mill in grinding process based on selective ensemble multi sensor information. *IEE, Transactions on Automation Science and Engineering* 10(3), pp. 726–740, DOI: 10.1109/TASE.2012.2225142.
- Tang et al 2014 – Tang, J., Chai, T., Cong, Q. Yuan, M., Zhao, L., Liu, Z. and Yu, W. 2014. Soft measurement of mill load parameters based on EMD and selective integrated learning algorithm. *Acta Automatica Sinica* 40(9), pp. 1853–1866, DOI: 10.3724/SP.J.1004.2014.01853.
- Torres et al. 2011 – Torres M.E., Colominas, M.A., Schlotthauer, G. and Flandrin, P. 2011. *A complete ensemble empirical mode decomposition with adaptive noise*. *IEEE International Conference on Speech and Signal Processing ICASSP*, Prague, Czech, pp. 4144–4147, DOI: 10.1109/ICASSP.2011.5947265.
- Wang et al. 2019 – Wang, H., Zhao, Y., Zhaohui, et al. 2019. Fault Diagnosis of Wind Turbine Gearbox based on EEMD Wavelet Threshold Denoising and CS-BP Neural Network. *Journal of Mechanical Transmission* 43(1), pp. 100–106.
- Wang et al. 2023 – Wang, R., Wang, Y.Z. and Lu, J. 2023. Photovoltaic power prediction based on ICEEMDAN-DTW and ISMA-WLSSVM. *Thermal Power Engineering* 38(9), pp. 131–140.
- Yang et al. 2015 – Yang W., Zhang P., Wang H., et al. 2015. Gear fault diagnosis based on multiscale fuzzy entropy of EEMD. *Journal of Vibration and Shock* 34(14), pp. 163–167+187.
- Zhao, L. 2014. Integrated modeling method for ball mill load parameters based on EEMD and PLS. Process Control Committee of Chinese Society of Automation. Committee of Process Control, Chinese Society of Automation. Proceedings of the 25<sup>th</sup> China Process Control Conference. Proceedings of the 25<sup>th</sup> China Process Control Conference. Process Control Committee of the Chinese Society of Automation: Chinese Society of Automation, pp. 8.
- Zhao et al 2017 – Zhao, L.J., Li, B., Wang, Y., et al. 2017. Mill Load Parameter Model Using Fast Decorrelated Neural Network Ensemble. *Control Engineering of China* 24(09), pp. 1952–1957.
- Zheng et al. 2014 – Zheng, J., Chen, M., Cheng, J. and Yang, Y. 2014. Multiscale fuzzy entropy and its application in rolling bearing fault diagnosis. *Journal of Vibration Engineering* 27(1), pp. 145–15.



- Zheng et al. 2016 – Zheng, J., Pan, H., Cheng, J., et al. 2016. Composite multi-scale fuzzy entropy based rolling bearing fault diagnosis method. *Journal of Vibration and Shock* 35(8), pp. 116–123.
- Zhu et al 2023 – Zhu J., Liu W., Gao L. 2023. Exploration and practice of intelligent mineral processing plant. *Non-ferrous Metals (Mineral Processing Section)* 1, pp. 121–126.

#### LOAD IDENTIFICATION METHOD OF BALL MILL BASED ON THE CEEMDAN-WAVELET THRESHOLD-PMMFE

##### Key words

mill load, bearing vibration signal, CEEMDAN-wavelet threshold, PMMFE, load identification

##### Abstract

In order to address the difficult problem of ball mill load identification during milling operation, the multi-scale fuzzy entropy algorithm is introduced into ball mill load identification and an innovative ball mill load identification method is proposed- the complete integrated empirical decomposition based on adaptive noise (CEEMDAN)-joint denoising with wavelet thresholding-multi-scale fuzzy entropy biased mean value (PMMFE) ball mill load identification method. Firstly, the vibration signals of ball mill bearings are denoised by the CEEMDAN-wavelet threshold joint denoising method and the analysis reveals that this method has obvious advantages over other denoising methods; secondly, the fuzzy entropy, multi-scale fuzzy entropy, and multi-scale fuzzy entropy deviation of denoised vibration signals are computed, the relationship between each entropy feature and the mill load is analysed in-depth and in an information-rich manner. Finally, the least squares support vector algorithm is used to identify the load of the feature vector. The analysis of the measured vibration signals reveals that the overall recognition rate of this method is 84.4%, which is significantly higher than that of other denoising methods and the combination of feature parameters, and the experiments show that the mill load recognition method based on CEEMDAN-wavelet thresholding-PMMFE is able to effectively identify the different loading states of ball mills.

#### METODA IDENTYFIKACJI OBCIĄŻENIA MLYNA KULOWEGO W OPARCIU O CEEMDAN – PRÓG FALKOWY –PMMFE

##### Słowa kluczowe

obciążenie młyna, sygnał drgań łożyska, próg CEEMDAN-fala, PMMFE, identyfikacja obciążenia

##### Streszczenie

W celu rozwiązania trudnego problemu identyfikacji obciążenia młyna kulowego podczas operacji mielenia, do identyfikacji obciążenia młyna kulowego wprowadzono wieloskalowy algorytm entropii rozmytej oraz zaproponowano innowacyjną metodę identyfikacji obciążenia młyna

kulowego – pełną zintegrowaną dekompozycję empiryczną opartą na szumie adaptacyjnym (CEEMDAN) – wspólne odsumianie z progowaniem falkowym – wieloskalowa metoda identyfikacji obciążenia młyna kulowego metodą rozmytej entropii z odchyleniem wartości średniej (PMMFE). Po pierwsze, sygnały wibracyjne łożysk młyna kulowego są odsumiane za pomocą wspólnej metody odsumiania CEEMDAN z progowaniem falkowym, a analiza pokazuje, że metoda ta ma oczywiste zalety w porównaniu z innymi metodami odsumiania; po drugie, obliczana jest rozmyta entropia, wieloskalowa rozmyta entropia i wieloskalowe rozmyte odchylenie entropii odsumionych sygnałów wibracyjnych, a związek między każdą cechą entropii a obciążeniem młyna jest analizowany dogłębnie i w sposób bogaty w informacje. Na koniec, algorytm wektora wsparcia najmniejszych kwadratów jest wykorzystywany do identyfikacji obciążenia wektora cech. Analiza zmierzonych sygnałów wibracyjnych pokazuje, że ogólny wskaźnik rozpoznawania tej metody wynosi 84,4%, co jest znacznie wyższe niż w przypadku innych metod odsumiania i kombinacji parametrów cech, a eksperymenty pokazują, że metoda rozpoznawania obciążenia młyna oparta na progowaniu falkowym CEEMDAN-PMMFE jest w stanie skutecznie identyfikować różne stany obciążenia młynów kulowych.